

Radar absorbing properties of polyvinyl alcohol/Ni–Zn ferrite-spinel composite

© V.G. Kostishyn, I.M. Isaev, R.I. Shakirzyanov, D.V. Salogub, A.R. Kayumova, V.K. Olitsky

National University of Science and Technology MISiS, Moscow, Russia
 e-mail: drvgkostishyn@mail.ru

Received July 16, 2021

Revised September 1, 2021

Accepted September 2, 2021

The electromagnetic and radio-absorbing characteristics of ferrite-polymer composites with conductive inclusions based on polyvinyl alcohol are investigated. The Ni–Zn spinel ferrite powder of 2000NN grade with composition $\text{Ni}_{0.32}\text{Zn}_{0.68}\text{Fe}_2\text{O}_4$ was used as filler. It is shown that the obtained composites are effective absorbers in the frequency range of 2–5 GHz with peak reflection loss less than ~ 20 dB. Through the analysis of the permittivity spectra and permeability spectra, as well as the calculated reflection loss spectra, critical factors of the electromagnetic wave absorption in obtained composites are established.

Keywords: polymer composite, radio absorption, nickel-zinc ferrite, polyvinyl alcohol

DOI: 10.21883/TP.2022.01.52540.217-21

Introduction

The wide use of satellite broadcasting, mobile telephony, and telecommunication systems in everyday life produces increased electromagnetic radiation (EMR) levels. Electromagnetic interference (EMI) and electromagnetic pollution caused by the elevated EMR background are among the most topical problems of the 21st century. EMI may shorten the lifetime and reduce the durability of electronic devices, and electromagnetic pollution may have a negative effect on vital activities of living organisms [1,2]. Materials for absorption or reflection of EMR are being researched actively to mitigate the EMI issues. Ferrite polymer composites (especially the ones based on ferrite spinels) are promising candidate materials for EMR absorption [3,4]. Ferrimagnetic materials feature high saturation magnetization, permittivity, and permeability, thus enhancing the losses of composite materials and radio absorption characteristics. Composites with a polymer matrix containing ferrites and semiconductors (graphene, metal nanoparticles) have marked radio absorption and radio screening properties induced by a combination of different absorption mechanisms: natural ferrimagnetic resonance (NFMR), domain-wall motion resonance (DWMR), eddy-current losses, repolarization losses, and multiple-reflection losses [5,6]. Since the NFMR frequency of ferrite spinels lies in the radio range that coincides with the operating frequencies of civilian EMR emitters, it is believed that composites with ferrite inclusions should be efficient absorbers in the civilian sector [7–12]. In addition, the microstructure specifics of polymer-based magnetic composites may have a considerable effect on the absorption spectra: the size, the shape, and the concentration of magnetic and conducting composites may alter the type

of frequency dispersion of permittivity and permeability and thus affect the frequency position of the absorption peak [13].

Polyvinyl alcohol (PVA) is a semi-crystalline polymer with a nonzero dipole moment and high permittivity [14]. Owing to its unique properties, PVA is widely used. In current research, it often serves as a biocompatible polymer matrix capable of encapsulating nanoparticles to avoid segregation. The radio absorption characteristics of PVA-based composites have already been studied. For example, PVA/reduced graphene oxide/carbonyl iron composites were produced in [15] by mixing fine iron powder with PVA and graphene oxide. These composites demonstrate fine absorption characteristics in the microwave band (reflection coefficient on a metal plate $R_l = -35$ dB at a frequency of 12 GHz and an absorption band (below -10 dB) of ~ 8 GHz). This is attributable to the presence of carbonyl iron (magnetic losses) and uniformly distributed graphene oxide (dielectric losses). It was demonstrated in other studies focused on PVA/carbon/Fe composites [16,17] that materials with high reflection losses in the 4–8 GHz frequency range with coefficient $R_l \sim -(20-30)$ dB may be produced. Marked screening properties were also observed for a flexible composite with barium hexaferrite nanodisks and soot introduced into a PVA matrix [18]. These composites have an attenuation index of 99.5% for electromagnetic waves within the 8–18 GHz frequency interval with predominant dielectric and magnetic losses.

In the present study, the electromagnetic characteristics of a ferrite polymer composite based on PVA and ferrite spinel (type 2000NN) powder are examined. The factors affecting absorption characteristics are also analyzed.

Table 1. Composition of experimental samples

Composition	Weight fraction of ferrite, %	Volume fraction of ferrite, %
PVA/Ni–Zn	20	5
PVA/Ni–Zn	40	13
PVA/Ni–Zn	60	25
PVA/Ni–Zn	80	47
PVA/Ni–Zn/Cu	60	25
PVA/Ni–Zn/graphite	80	47

1. Objects under study and experimental procedure

Experimental samples were prepared by pressing a mixture of powders under heating. Ferrite spinel type 2000NN with the $\text{Ni}_{0.32}\text{Zn}_{0.68}\text{Fe}_2\text{O}_4$ composition was used as a filler for composites. Sintered Ni–Zn ferrite products were ground up in a mill into ferrite powder (fraction $< 45\ \mu\text{m}$). Polymer powder type PVA 16/1 was used as the matrix. Powders were premixed to a uniform mixture and introduced into a mold. Samples were fabricated in the form of rings with an outer diameter of 16 mm, inner diameter of 7 mm, and height $d = 5\text{--}7.5\ \text{mm}$ by holding them for 5 min at 150 MPa and a temperature of 190°C.

Complex permeability μ_r^* , permittivity ε_r^* , and spectra of reflection coefficient on a metal plate R_l within the 0.01–7 GHz frequency range were measured using a coaxial cell and a Rohde & Schwartz ZVL-13 vector network analyzer.

The composition of the obtained samples is detailed in Table 1. Copper foil and graphite type GK-1 (resistivity: $4.5 \cdot 10^{-3}\ \Omega\cdot\text{m}$) were used as a conducting additive for composites with weight fractions of 60 and 80%, respectively. Copper foil was obtained by delamination of films with a thickness of $\sim 2\ \mu\text{m}$ from glass substrates and added to the mixture of ferrite and polymer powders. Its weight fraction was 3%. The weight fraction of graphite GK-1 was 5%.

2. Experimental results

Figure 1 shows the spectra of permittivity $\varepsilon_r'(f)$ of the experimental composite samples, pure PVA, and Ni–Zn ferrite. It can be seen that the real part of permittivity increases with ferrite concentration. None of the experimental samples revealed any pronounced dispersion of permittivity spectra in the 0.05–7 GHz region. A „tail,“ which may correspond to different polarization mechanisms, is seen below this region. It is known that crystals with ionic bonding of the MeFe_2O_4 spinel ferrite type feature two mechanisms of ion polarization: polarization due to charge shift and hopping polarization (due to interstitial ion migration). The first mechanism arises at high frequencies ($10^{12}\text{--}10^{15}\ \text{GHz}$) and characterizes the material properties [19]. The second

mechanism is related to the defect structure of the crystal lattice when interstitial ions migrate over long distances (on the order of the interatomic distance) under the influence of thermal fluctuations of the lattice. This mechanism operates at lower frequencies ($10^4\text{--}10^7\ \text{Hz}$) and should manifest itself in ferrite ceramics due to the presence of Frenkel defects and complex structure (polycrystalline grains and vitreous grain boundaries). Ground ferrite (after milling) is likely to have a higher density of defects than the initial ferrite ceramic. This should translate into high dielectric losses, but the spectra of the dielectric loss tangent ($\tan \delta_\varepsilon = \varepsilon_r''/\varepsilon_r'$ in the inset of Fig. 1) suggest otherwise. The dielectric loss tangent for all composites does not exceed 0.2, while the corresponding value for the unmilled ceramic bulk Ni–Zn sample is almost 0.6.

The complex structure of ceramic ferrite is conducive to the formation of space charges between high-resistance grain boundaries and low-resistance grains. Owing to hopping conductivity in ferrites between Me^{2+} and Me^{3+} ions (sites A and B), electrons or holes accumulate at the interfaces between grains and grain boundaries and form space charges [20,21]. Maxwell–Wagner relaxation is observed in this context at low frequencies (below several MHz). It was demonstrated in [22,23] that the dispersion of permittivity within the 1–10 MHz frequency interval may be related to a different mechanism wherein the frequency of electron jumps between Fe^{2+} and Fe^{3+} coincides with the frequency of the applied field, as is the case in Cu–Zn or Mn–Zn ferrites (and, probably, the $\text{Ni}_{0.32}\text{Zn}_{0.68}\text{Fe}_2\text{O}_4$ ferrite ceramic examined in the present study). The permittivity spectra of high-resistance PVA/Ni–Zn ferrite composites suggest that no relaxation processes occur in the 0.05–7 GHz interval. The shape of permittivity spectra and the high dielectric loss tangent for the initial sintered bulk Ni–Zn ferrite sample may be attributed to the above mechanisms. As for the semi-crystalline PVA matrix, all molecular dynamics relaxation processes transpire in the low-frequency region and do not reveal themselves in the 0.05–7 GHz range [24].

The dependence of the conductivity at a frequency of 1 GHz on the ferrite concentration is presented in Fig. 1, b. It can be seen that the conductivity varies little with ferrite concentration, but the addition of graphite results in a twofold increase in σ . The relatively high conductivity of unmilled ferrite ceramic 2000NN is attributable to the presence of marked relaxation processes. It should be noted that a small admixture of Cu microfoil does not enhance the conductivity of the PVA/Ni–Zn composite. This is likely related to the small thickness of foil and the low concentration (well below the percolation threshold).

The spectra of permeability $\mu_r'(f)$, $\mu_r''(f)$ (Fig. 2) also demonstrate that the average value of complex permeability increases with ferrite concentration. The permeability spectra for all compositions in the 0.1–1 GHz frequency range are characterized by marked dispersion related to two mechanisms: DWMR (low-frequency region) and spin rotation

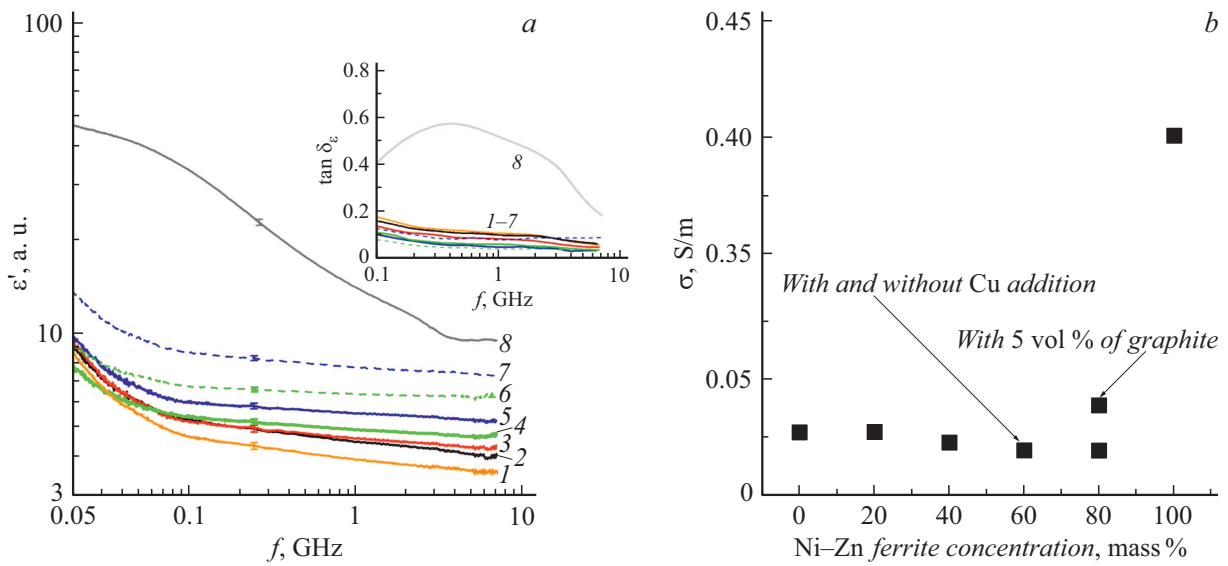


Figure 1. *a* — permittivity spectra, *b* — dependence of conductivity on the concentration of ferrite. Spectra of the dielectric loss tangent are shown in the inset. 1 — PVA, 2 — 20% PVA/Ni-Zn, 3 — 40% PVA/Ni-Zn, 4 — 60% PVA/Ni-Zn, 5 — 80% PVA/Ni-Zn, 6 — 60% PVA/Ni-Zn and Cu, 7 — 80% PVA/Ni-Zn, 8 — bulk sintered ceramic ferrite.

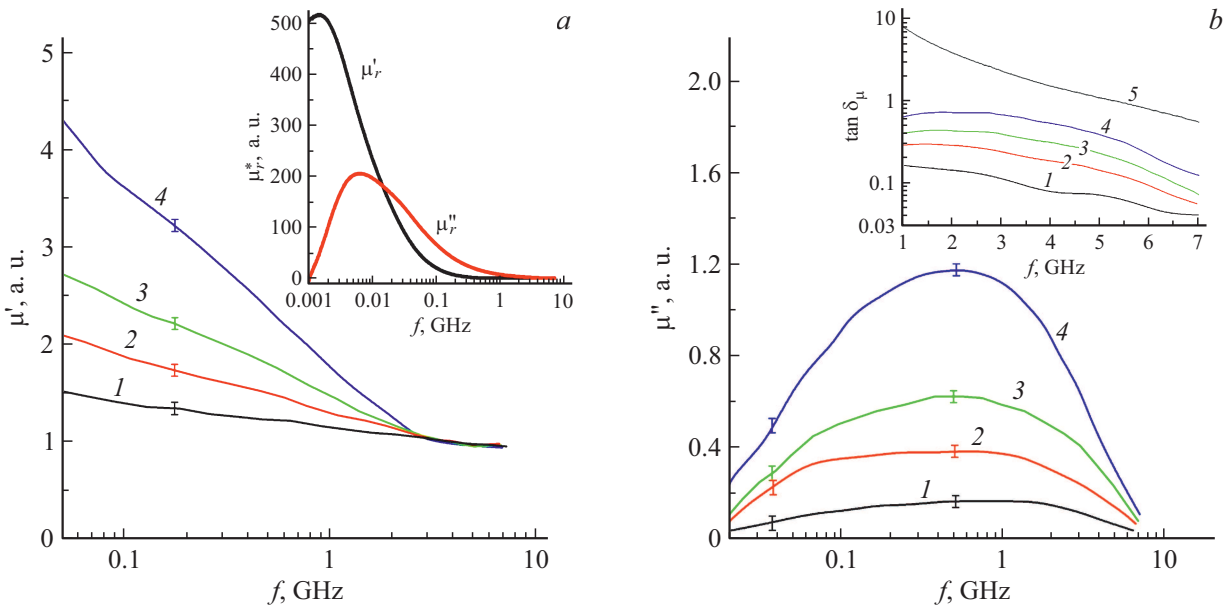


Figure 2. Spectra of real (*a*) and imaginary (*b*) parts of permeability; complex permeability spectra for sintered Ni-Zn ceramic ferrite and spectra of the magnetic loss tangent are shown in the insets. 1 — 20% PVA/Ni-Zn, 2 — 40% PVA/Ni-Zn, 3 — 60% PVA/Ni-Zn, 4 — 80% PVA/Ni-Zn, 5 — bulk ceramic Ni-Zn ferrite.

(NFMR, high frequency) [25]. Significant differences in permeability of composites with a ferrite weight fraction of 20 and 80% (and pure bulk ceramic ferrite) are attributable to the magnetic flux discontinuity in composites with a low weight fraction. As the concentration of ferrite increases, the magnetic flux intensifies, thus raising the permeability. It should be noted that high-conductivity admixtures do not alter the permeability. The marked difference in dispersion frequencies of ferrite ceramic and composites (see Fig. 2, *a* and the inset) is another feature of $\mu_r'(f)$, $\mu_r''(f)$ spectra.

First, since small-sized ferrite particles in a composite do not contain a large number of magnetic domains, low-frequency maxima of $\mu_r''(f)$, which are caused by the motion of domain walls, do not manifest themselves in the spectra of composites. Second, the natural resonance frequency defined as $\omega_{\max} = H_{\text{eff}} \cdot 4\pi M_s$ depends strongly on the magnetic anisotropy or on the effective field of magnetic anisotropy H_{eff} [26]. The key factors affecting the value of H_{eff} are crystalline magnetic anisotropy, magnetic-dipole anisotropy (demagnetizing fields), elastic stress anisotropy

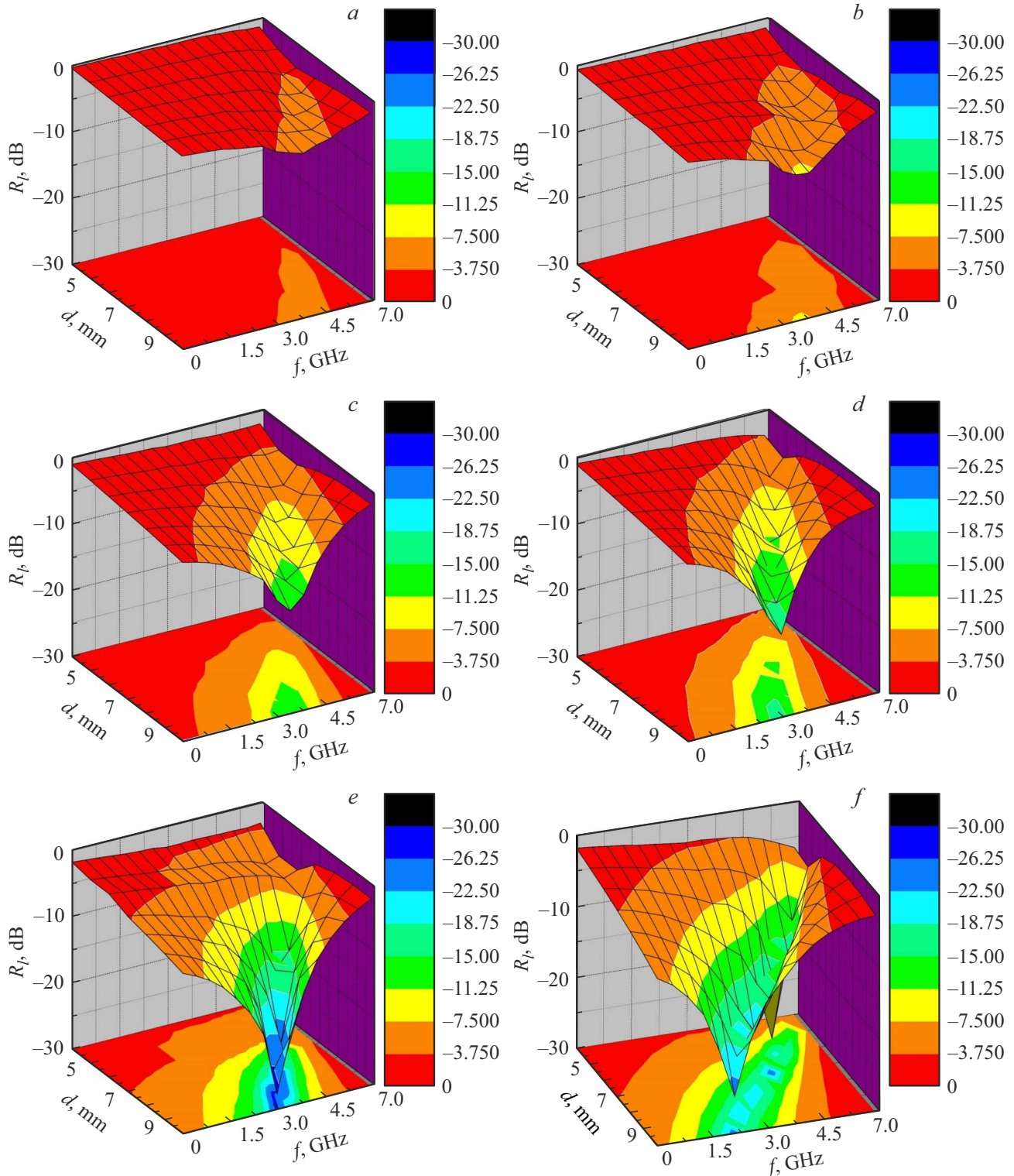


Figure 3. Three-dimensional surfaces of the reflection coefficient on a metal plate for the obtained composites: *a* — 20% PVA/Ni–Zn, *b* — 40% PVA/Ni–Zn, *c* — 60% PVA/Ni–Zn, *d* — 60% PVA/Ni–Zn and Cu, *e* — 80% PVA/Ni–Zn, *f* — 80% PVA/Ni–Zn and graphite.

(magnetoelastic anisotropy or magnetostriction anisotropy), shape anisotropy, surface magnetic anisotropy, etc. [27]. The shift of the NFMR frequency toward higher frequencies may be attributed to the influence of demagnetizing fields emerging when a nonmagnetic interlayer is introduced

between magnetic particles. These internal demagnetizing fields alter the distribution of magnetization within the material and enhance H_{eff} .

Magnetic loss tangent $\tan \delta_{\mu} = \mu''/\mu'_r$ in the 1–7 GHz frequency interval is presented in the inset of Fig. 2, *b*. It

Table 2. Comparison of the absorption parameters of experimental and calculated $R_I(f)$ spectra with a normalized impedance and an interference thickness

Sample	Weight fraction of ferrite, %	d , mm	Z_{in}/Z_0	t_m , mm	f_0 , GHz	$ R_I^{max} $, dB	Δf , GHz
PVA/Ni–Zn	20	7.0	3.38	6.50	5.65	4.5	–
PVA/Ni–Zn	40	6.0	2.91	6.50	5.65	5.6	–
PVA/Ni–Zn	60	7.0	1.80	6.15	5.86	9.2	–
PVA/Ni–Zn	80	7.0	1.14	7.76	4.46	22.6	2.4
PVA/Ni–Zn	60	10.0	1.47	10.3	3.71	14.6	1.2
PVA/Ni–Zn/Cu	60	10.0	1.33	10.4	2.76	18.4	1.2
PVA/Ni–Zn/graphite	80	6.0	1.02	6.0	5.13	33.7	2.3

can be seen that the value of $\tan \delta_\mu$ reaches 0.6–0.8 in composites with a high weight fraction of Ni–Zn ferrite (60 and 80 mass.%), while $\tan \delta_\mu$ in the initial ferrite ceramic decreases from 10 to 1. The permeability spectra suggest that magnetic losses are higher in materials with a high concentration of the magnetic phase. This is the reason why $\tan \delta_\mu$ of ferrite ceramics is considerably higher than that of PVA/Ni–Zn composites. It follows from the comparison of $\tan \delta_\mu$ and $\tan \delta_\epsilon$ in the 1–7 GHz range that the magnetic losses are dominant in the obtained PVA/Ni–Zn composites.

All the polarization and magnetic resonance processes mentioned above contribute to electromagnetic radiation energy losses in composites. The absorption characteristics of composites were estimated based on the value of reflection coefficient on a metal plate R_I . Calculated R_I spectra were obtained using formulae (1) and (2) and the spectra of permittivity and permeability:

$$R_I = 20 \log \left| \frac{Z_{in} - Z_0}{Z_{in} + Z_0} \right|, \quad (1)$$

$$Z_{in} = Z_0 \sqrt{\frac{\mu_r^*}{\epsilon_r^*}} \tanh \left[j \frac{2\pi f d}{c} \sqrt{\mu_r^* \epsilon_r^*} \right], \quad (2)$$

where Z_0 is the free space impedance, d is the absorber thickness, and c is the speed of light.

Three-dimensional surfaces of reflection coefficient on a metal plate R_I are presented in Fig. 3. It can be seen from Figs. 3, *a* and 3, *b* that no significant losses are observed in composites with a ferrite weight fraction of 20% and 40% and the thickness varying within the 4–10 mm interval. An intriguing result was obtained for the 60% PVA/Ni–Zn composite. The peak absorption increases from –14.6 to –18.3 dB after the introduction of a small fraction of copper foil. It is not improbable that 2D conducting objects present in the composite structure form local regions of multiple reflection, thus enhancing the electromagnetic energy losses. Similar results were obtained in [28] where hollow microspheres (cenospheres) coated with Ag nanoparticles were introduced into a polypyrrole matrix. PVA/Ni–Zn and PVA/Ni–Zn/graphite composites with 80 mass.% of ferrite exhibit fine absorption characteristics at a thickness

of 8–10 and 6–10 mm, respectively. It is crucial to reduce the mass and dimensional parameters of absorbers (especially for military applications). In view of this, the PVA/Ni–Zn/graphite composite is more practical, since it has low values of the reflection coefficient on a metal plate (below –10 dB) at a thickness of 5–10 mm.

The spectra of $R_I(f)$ for different samples were compared to identify the factors affecting losses in reflection on a metal plate (Table 2). The obtained results demonstrate that the matching condition of impedances ($Z_{in}/Z_0 = 1$) and interference thickness $t_m \approx d$ are fulfilled in absorbers with high $|R_I^{max}|$ values [29,30]. Strong absorption in composites is induced by magnetic losses and the matching of impedances and thickness $t_m = c/4f \sqrt{|\mu_r^* \epsilon_r^*|}$ (when the absorber thickness is equal to the calculated interference thickness $t_m \sim \lambda/4$). If these conditions are fulfilled, the angular difference of phases of electromagnetic waves reflected from the sample surface and from the metal surface is $\pi/2$. It can be seen from Table 2 that none of these conditions are fulfilled for PVA/Ni–Zn composites with a ferrite weight fraction of 20, 40%. This is the reason why the reflection coefficient is low. The considerable width Δf of the –10 dB absorption (i.e., absorption of 90% of energy) band in the obtained composites is also of note. This band width for the calculated spectra of composites with 80% of ferrite is ~ 2.3 GHz. If conducting inclusions are introduced into composites with Ni–Zn ferrite, an increase in $|R_I|$ and a reduction in the matching thickness are expected. This is attributable to an increase in conduction losses (eddy currents) in the PVA/Ni–Zn/graphite composite. In addition, frequency f_0 of the maximum absorption shifts toward lower frequencies as the ferrite concentration increases.

Conclusion

The obtained PVA/Ni_{0.32}Zn_{0.68}Fe₂O₄ composites were characterized by high-frequency measurements of their permittivity and permeability. The permittivity spectra do not reveal any marked dispersion due to dielectric relaxation processes in the 0.05–7 GHz range. Dispersion from

NFMR and DWMR was observed in measurements of the dynamic permeability. High peak values of the reflection coefficient on a metal plate (below -10 dB in the 2–5 GHz frequency interval at a thickness of 6–10 mm) were calculated for composites with high ferrite concentrations (60, 80%). Magnetic losses are dominant in composites with Ni–Zn ferrite only. The introduction of conducting admixtures into PVA/Ni–Zn composites may result in enhancement of their absorption characteristics due to eddy-current and multiple-reflection losses. It was demonstrated that high absorption characteristics in composites are the result of fulfillment of the impedance matching condition and correspondence between the absorber thickness and the calculated interference thickness.

Funding

This study was supported by a grant from the Russian Science Foundation (agreement No. 19-19-00694 dated May 6, 2019).

Conflict of interest

The authors declare that they have no conflict of interest.

References

- [1] D. Wanasinghe, F. Aslani. *Composites Part B*, **176**, 107207 (2019). DOI: 10.1016/j.compositesb.2019.107207
- [2] E.V. Yakushko, L.V. Kozhitov, D.G. Muratov, E.Yu. Korovin, A.A. Lomov, A.V. Popkova. *Russ. Phys. J.*, **63** (12), 2226 (2021). DOI: 10.1007/s11182-021-02292-8
- [3] D. Kumar, A. Moharana, A. Kumar. *Mater. Today Chem.*, **17**, 100346 (2020). DOI: 10.1016/j.mtchem.2020.100346
- [4] S.B. Narang, K. Pubby. *J. Magn. Magn.*, **519**, 167163 (2021). DOI: 10.1016/j.jmmm.2020.167163
- [5] X. Zeng, X. Cheng, R. Yu, G.D. Stucky. *Carbon*, **168**, 606 (2020). DOI: 10.1016/j.carbon.2020.07.028
- [6] Z.W. Li, G.Q. Lin, Linfeng Chen, Y.P. Wu, C.K. Ong. *J. Appl. Phys.*, **98**, 094310 (2005). DOI: 10.1063/1.2128688
- [7] V.G. Andreev, S.B. Menshova, A.N. Klimov, R.M. Vergazov, S.B. Bibikov, M.V. Prokofiev. *J. Magn. Magn.*, **394**, 1 (2015). DOI: 10.1016/j.jmmm.2015.06.007
- [8] R.I. Shakirzyanov, V.G. Kostishyn, A.T. Morchenko, I.M. Isaev, V.V. Kozlov, V.A. Astakhov. *Russ. J. Inorg. Chem.*, **65** (6), 829 (2020). DOI: 10.1134/S0036023620060194
- [9] V.G. Kostishin, R.M. Vergazov, S.B. Men'shova, I.M. Isaev, A.V. Timofeev. *Zavod. Lab., Diagn. Mater.*, **87** (1), 30 (2021) (in Russian). DOI: 10.26896/1028-6861-2021-87-1-30-34
- [10] V.G. Kostishin, R.M. Vergazov, S.B. Men'shova, I.M. Isaev. *Russ. Tekhnol. Zh.*, **8** (6), 87 (2020) (in Russian). DOI: 10.32362/2500-316X-2020-8-6-87-108
- [11] I.M. Isaev, V.G. Kostishin, V.V. Korovushkin, D.V. Salogub, R.I. Shakirzyanov, A.V. Timofeev, A.Yu. Mironovich. *Zh. Tekh. Fiz.*, **91** (9), 1376 (2021) (in Russian). DOI: 10.21883/JTF.2021.09.51217.74-21
- [12] M.A. Almessiere, Y. Slimani, A.V. Trukhanov, A. Baykal, H. Gungunes, E.L. Trukhanova, S.V. Trukhanov, V.G. Kostishin. *J. Ind. Eng. Chem.*, **90**, 251 (2020). DOI: 10.1016/j.jiec.2020.07.020
- [13] A.V. Lopatin, N.E. Kazantseva, Y.N. Kazantsev, O.A. D'yakonova, J. Vilčková, P. Sába. *J. Commun. Technol. Electron.*, **53** (5), 487 (2008). DOI: 10.1134/S106422690805001X
- [14] M. Aslam, M.A. Kalyar, Z.A. Raza. *Polym. Eng. Sci.*, **58**, 2119 (2018). DOI: 10.1002/pen.24855
- [15] Zhang Qi, Liu Chunbo, Wu Zhuang, Yang Yang, Xie Zhiyong, Zhou Haikun, Chen Chudong. *J. Magn. Magn.*, **479**, 337 (2019). DOI: 10.1016/j.jmmm.2018.11.129
- [16] Y.K. Lahsmin, H. Heryanto, S. Ilyas, A.N. Fahri, B. Abdullah, D. Tahir. *Opt. Mater.*, **111**, 110639 (2021). DOI: 10.1016/j.optmat.2020.110639
- [17] B. Abdullah, S. Ilyas, D. Tahir. *J. Nanomater.*, **2018**, 9823263 (2018). DOI: 10.1155/2018/9823263
- [18] S. Kumar, G. Datt, A.S. Kumar, A.C. Abhyankar. *J. Appl. Phys.*, **120**, 164901 (2016). DOI: 10.1063/1.4964873
- [19] M.T. Sebastian. *Dielectric Materials for Wireless Communication* (Elsevier, Amsterdam, Boston, 2008)
- [20] R. Metselaar, P.K. Larsen, in *Proceedings of the International School of Physics Enrico Fermi* (1978), v. 70, p. 417.
- [21] V.G. Kostishin, R.I. Shakirzyanov, A.G. Nalogin, S.V. Shcherbakov, I.M. Isaev, M.A. Nemirovich, M.A. Mikhailenko, M.V. Korobeinikov, M.P. Mezentseva, D.V. Salogub. *Phys. Solid State*, **63**, 435 (2021). DOI: 10.1134/S1063783421030094
- [22] J. Parashar, V.K. Saxena, J. Sharma, D. Bhatnagar, K.B. Sharma. *Macromol. Symp.*, **357** (1), 43 (2015). DOI: 10.1002/masy.201400184
- [23] P. Pengfei, Z. Ning. *J. Magn. Magn.*, **416**, 256 (2016). DOI: 10.1016/j.jmmm.2016.05.018
- [24] N. Ghorbel, A. Kallel, S. Boufi. *Composites Part A*, **124**, 105465 (2019). DOI: 10.1016/j.compositesa.2019.05.033
- [25] S.B. Narang, K. Pubby. *J. Magn. Magn.*, **519**, 167163 (2021). DOI: 10.1016/j.jmmm.2020.167163
- [26] S. Chikazumi, C.D. Graham. *Physics of Ferromagnetism, 2nd ed.* (Clarendon Press, Oxford University Press, Oxford, NY, 1997)
- [27] V. Babayan, N.E. Kazantseva, R. Moučka, I. Sapurina, Yu.M. Spivak, V.A. Moshnikov. *J. Magn. Magn.*, **324** (2), 161 (2012). DOI: 10.1016/j.jmmm.2011.08.002
- [28] R. Panigrahi, S. Srivastava. *Sci. Rep.*, **5**, 7638 (2015). DOI: 10.1038/srep07638
- [29] B. Wang, J. Wei, L. Qiao, T. Wang, F. Li. *J. Magn. Magn.*, **324**, 761 (2012). DOI: 10.1016/j.jmmm.2011.09.011
- [30] Tao Wang, Rui Han, Guoguo Tan, Jianqiang Wei, Liang Qiao, Fashen Li. *J. Appl. Phys.*, **112**, 104903 (2012). DOI: 10.1063/1.4767365